

See discussions, stats, and author profiles for this publication at: <https://www.researchgate.net/publication/328179903>

# Evolution of the statistical fluctuations in the measured temperature differences between painted metal plates of a CUBI infrared calibration target

Conference Paper · October 2018

DOI: 10.1117/12.2325255

CITATIONS

0

READS

27

3 authors, including:



Gareth Dafydd Lewis

Royal Military Academy

21 PUBLICATIONS 235 CITATIONS

[SEE PROFILE](#)

Some of the authors of this publication are also working on these related projects:



Radar writings [View project](#)



Infrared Polarimetric Imaging [View project](#)

# PROCEEDINGS OF SPIE

[SPIDigitalLibrary.org/conference-proceedings-of-spie](https://spiedigitallibrary.org/conference-proceedings-of-spie)

## Evolution of the statistical fluctuations in the measured temperature differences between painted metal plates of a CUBI infrared calibration target

G. D. Lewis, P. Merken, M. Vandewal

G. D. Lewis, P. Merken, M. Vandewal , "Evolution of the statistical fluctuations in the measured temperature differences between painted metal plates of a CUBI infrared calibration target," Proc. SPIE 10794, Target and Background Signatures IV, 1079408 (9 October 2018); doi: 10.1117/12.2325255

**SPIE.**

Event: SPIE Security + Defence, 2018, Berlin, Germany

# Evolution of the statistical fluctuations in the measured temperature differences between painted metal plates of a CUBI infrared calibration target

G.D. Lewis\*, P Merken, M. Vandewal  
Royal Military Academy, CISS Department, Renaissancelaan 30, 1000 Brussels, Belgium;

## ABSTRACT

To validate thermal infrared signature models, we need data from well-characterized targets, typically of simple geometric shape measured under known atmospheric and environmental conditions. An important parameter of the target's signature is the variability in surface temperature due to an orientation with regard to the dominant heat source: the sun. In this paper, we report on the fluctuations in the temperature differences between surfaces of a CUBI geometrical test target mounted at roof level in an urban environment. Specifically, we investigate those surfaces orientated in a step-like manner. Measurements are recorded at regular intervals by digital temperature sensors operating in a network and remotely accessed via intranet. Our results assess the statistical variation in relative temperature contrast between surfaces for the entire dataset, where queries to a database highlight patterns in the data. We show not only a pronounced difference in probability density functions due to the influence of the sun by day and radiative cooling by night, but also the statistical variability of the temperature differences with local time. In summary, we show statistical limits on the probable temperature differences between plates as a function of time of day over a number of months, which provide a useful insight to the IR signature.

**Keywords:** IR signatures, CUBI, temperature measurements, signature monitoring

## 1. INTRODUCTION

The temperature signature of a well-characterized target such as the CUBI, is an essential component in the validation of infrared (IR) signature models and simulations<sup>1</sup>. This simple geometric shape of known thermal and optical properties, permits us to understand the influence of the environment and atmosphere on the temperature and radiometric properties observed by an IR imaging system.

Willers et al.<sup>1</sup>, stated that a test target such as the CUBI is of great interest to help validate signature models. van Iersel et al.<sup>2</sup> demonstrated the influence of environmental change on the temperature of facets of the CUBI. They proved that the solar irradiance and the exchange of energy to the surroundings accounts for the evolution of temperature from plates of the target. In another study, researchers highlighted yet again the usefulness of the CUBI for both the development and the validation of thermal infrared models<sup>3</sup>. Recently, the target was used to investigate the dynamic temperature variations using wavelet analysis<sup>4</sup>. It is necessary to include dynamic signature fluctuations in order to make IR predictive models real-time and representative<sup>5</sup>.

In addition to understanding the dynamic temperature fluctuations to improve the realism of predictive models, it is also important to appreciate how our dataset could be used to support other aspects of IR signature management. For example, in the standards, requirements and specifications for above water signatures of ships. If we consider an equivalence to IR camouflage specifications<sup>6</sup>, then the spatial variation of the temperature the target is very important for IR signature management.

\* [gareth.lewis@rma.ac.be](mailto:gareth.lewis@rma.ac.be); phone: 32 2 44 14200; fax: 32 2 44 39187; <http://sic.rma.ac.be>

The objective of this article, is to query a database of temperature measurements from the CUBI so as to provide a statistical analysis of the fluctuations in temperature differences between plates; in particular, we analyse those plates aligned along the ‘L’ shaped step of the CUBI calibration target. In doing so, we provide a technique where we can continuously probe our data with queries for further analysis. In the subsequent sections, this article presents an overview of the experimental arrangement with focus on the analysis methods. In the results section, we explore the importance of differences in temperature between neighbouring CUBI plates to understand temperature and thermal contrast. Finally, we present conclusions and outline a route for further research.

## 2. METHODS

The experimental arrangement focuses on the CUBI geometrical L-shaped target painted in naval grey<sup>7</sup>.

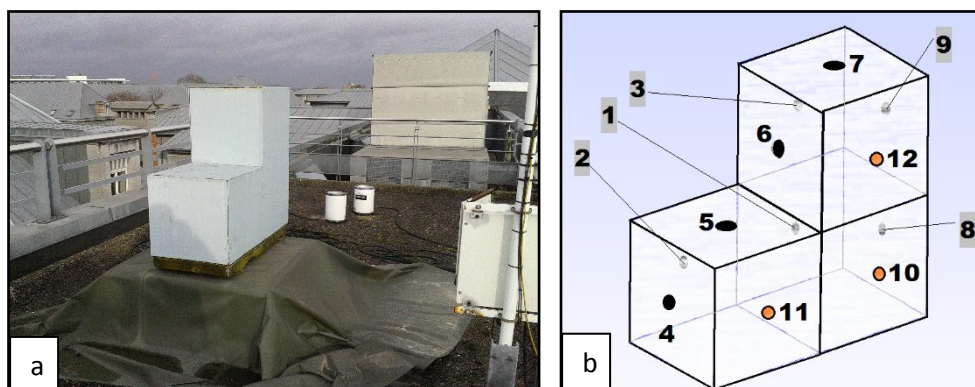


Figure 1, The CUBI situated on the roof site facing due South in (a), and a sketch diagram highlighting the position and number identity of the temperature sensors in (b). Note, we designate the plates 4, 5, 6 and 7 as the ‘step’ in this article.

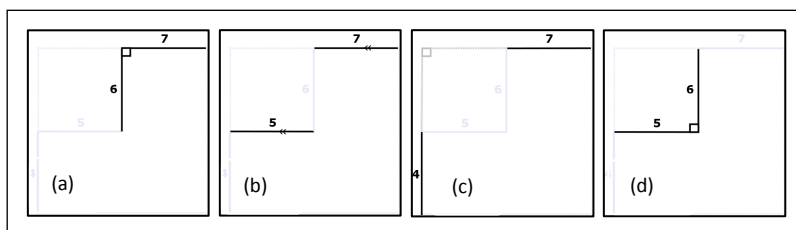


Figure 2, the set of four CUBI plate pairs that will be used throughout our results to explore the differences in surface temperature along the CUBI ‘step’.

### 2.1 CUBI Geometrical object

The CUBI can be thought of as three identical cubes placed in an L-shaped step (Figure 1). It consists of a 4 mm steel outer shell painted with primers, flat coats and finished in naval gray. Inside the CUBI, a sandwich of 5 cm thick polyurethane foam and 2 cm thick plywood insulates the inner part of the shell. At the center of each face is a temperature probe mounted from the inside, where the numbers refer to the plate's location that will be used to identify the results (Figure 1b). Temperature data from the sensors are sent along a network to a microcontroller accessible from our local intranet. The combination of plates used in the analysis is shown in Figure 2, where a difference in the temperatures of the two plates will be measured. Three of the combinations of plates (Figures 2a, b and c) reference their temperatures with respect to plate 7 (top horizontal plate), while the last combination (Figure 2d) investigates the interaction of the orthogonal plates 6 and 5. The latter combination explores the internal right-angle of the ‘step’.

The CUBI was built in 2007 and placed on our roof laboratory with the ‘L’ shape facing due South. In December 2014, the temperature sensors were upgraded from thermocouples to digital networked temperature probes. The trial period covered in this article was from May to early December 2015.

## 2.2 Digital Temperature Sensors

Fourteen DS18B20 temperature sensors are located inside the CUBI, twelve fixed to the inside of the plates, and two as internal references<sup>8</sup>. The sensor is a digital thermometer that provides 9-bit to 12-bit temperature measurements over a range from  $-55^{\circ}\text{C}$  to  $+125^{\circ}\text{C}$ . Each device has a unique 64-bit serial code, which permits many devices to communicate over a 1-wire bus. The accuracy of the sensors was improved from  $\pm 0.5^{\circ}\text{C}$  to approximately  $\pm 0.02^{\circ}\text{C}$  after calibration with a WEISS 180 climate chamber for the range of temperatures from  $-20^{\circ}\text{C}$  to  $+50^{\circ}\text{C}$ . The temperature resolution was fixed at 11-bit, giving increments of  $0.125^{\circ}\text{C}$ . This is a compromise between the time necessary to convert a temperature to a digital word of 375ms with respect to the desired to the resolution in temperature. This compares with 93.75ms for 9-bit ( $0.5^{\circ}\text{C}$ ) up to 750ms for 12-bit ( $0.0625^{\circ}\text{C}$ ).

The raw data from all sensors report a continuous temperature stream every 18 seconds to a microcontroller via a network, which results in approximately 4800 records per channel per day. This gives a total number of records close to one million over the whole period of the trial.

## 2.3 Data Analysis

The central aspect of our data analysis is the expression of a normalized relational database of sensor temperature records that then was queried. A schematic (Figure 3) shows that the database (PostgreSQL) is created from the corrected temperature records using individual calibrations for each device. Queries were created in the database via Python programming scripts calling SQL libraries.

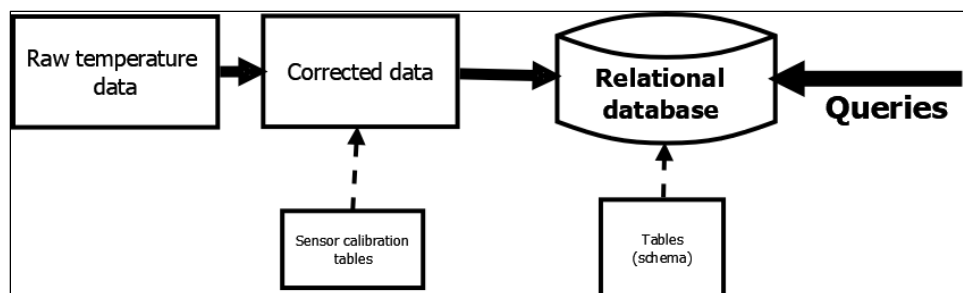


Figure 3, the schematic of the data analysis process, indicating the route from raw data to a relational database that then could be queried.

## 3. RESULTS AND DISCUSSION

In this section, we present the results of the variation in surface temperature for plates along the step of the CUBI (Figure 1 and Figure 2). Our trials ran from May to December in 2015, and amounted to approximately 180 days of measurements for all plates.

The results are divided into three subsections: 3.1) examples of the differences in temperature between plates for three selected days over the period, 3.2) the temperature difference between two plates for all datasets characterized by month over the whole data set and 3.3) the probability density functions for the difference in surface temperatures between the ‘step’ plate combinations for day and night separately.

### 3.1 Diurnal temperature variability for selected days

In the graphs on the top row of Figure 4, we demonstrate the variability of the temperature for the plates along the L-shaped step of the CUBI for three selected days of different meteorological conditions, which are typical of results reported by other researchers<sup>2,3,9</sup>. The selected days cover the period of our data set from May to December. Notice, the significant differences between Figure 4(1) and 4(2). On the bottom row of graphs, we display the difference in temperature between the step plates for the combinations shown in Figure 2. For example, the legend name DTp7m6, represents the temperature difference between two plates 7 and 6.

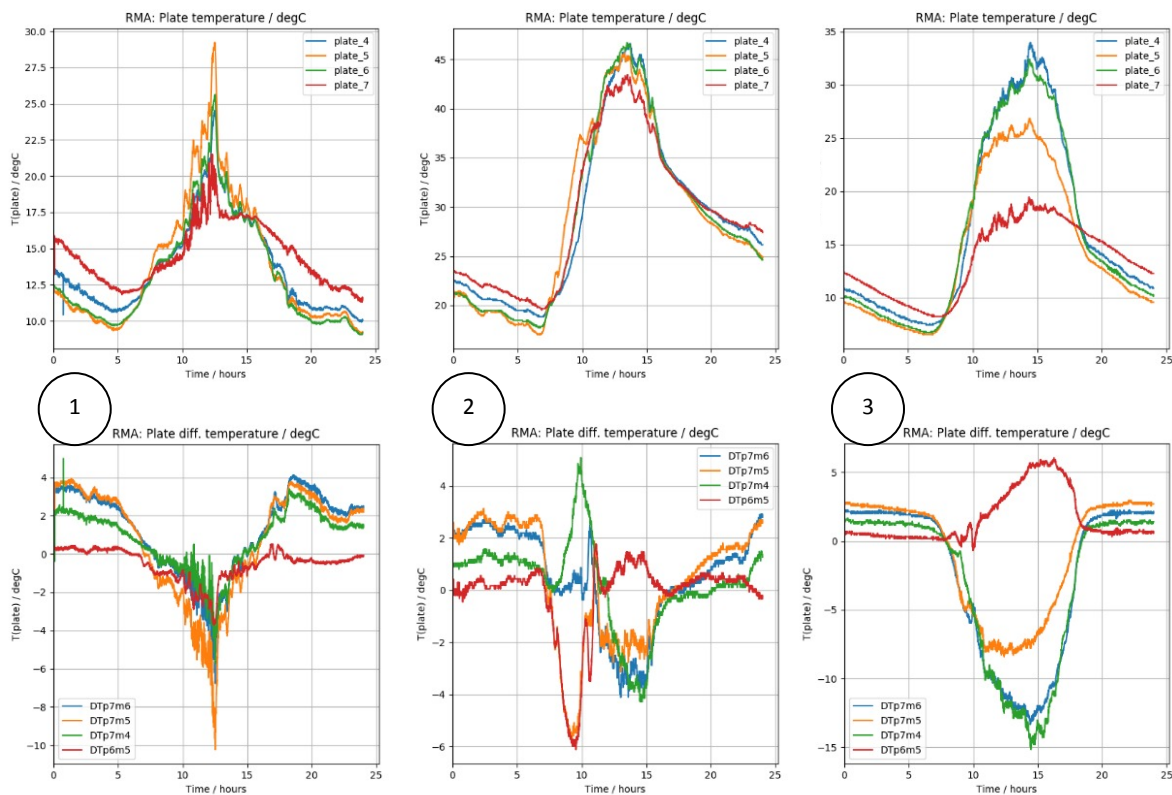


Figure 4, the diurnal variation of the CUBI plate temperatures (top row) together with the variation of the temperature difference between the plates (bottom row) for three days during the trial: 1) 29th May 2015, 2) 30th August 2015 and 3) 30th September 2015. The legend on the bottom row shows the combination of plates as given in Figure 2. For example, DTp7m6 represents the plates for Figure 2a, the temperature difference between plates 7 and 6.

Figure 4 also highlights, just as for all our data set, that it is highly improbable that any two days of measurements would be identical, and that by looking at the temperature differences between plates we stress a useful additional discriminant for IR signature management. The peak temperatures for all plates along the step (orientated South) were as predicted to be a maximum in the early afternoon. Note, that the top horizontal plate of the CUBI (plate 7) gives the lowest maximum at midday, but the highest temperatures during the night. In particular on Figure 4(3), where the difference in peak day temperature is nearly 15°C between plate 4 and plate 7.

In all the step combinations, the temperature difference between plate 6 and plate 5 results in the lowest; although, not zero as may be first suspected. Notice the obvious thermal crossover period where all plates have a similar temperature.

This occurs twice during the day, at around the time of sunrise and sunset with the morning crossover normally more pronounced. Note that the temperature differences do allow us a better appreciation of how the relative signatures between plates change throughout the daytime irrespective of the absolute temperature.

### 3.2 Diurnal variability of temperature difference over the entire dataset

A description of the temperature variability of the CUBI plates over a day is typically limited to an analysis of only a few consecutive days showing how the predicted model fits the real data; even though, this may have come from a larger data set that could have been used to understand statistical aspects of the data<sup>2,3</sup>.

In Figure 5 we show how the temperature differences vary diurnally for the whole period, representing about 800,000 records per sensor over that period. Each data point is color coded by month. We queried the database with the following question in mind, 'what is the temperature contrast between plates as a function of the month?' Each of the sub-graphs in Figure 5 corresponds to the set of CUBI plate pairs as previously shown in Figure 2. To aid clarity, we add also a small graphic showing the relevant plate numbers. For example, Figure 5a explores the difference in temperature between plates 7 and 6.

In general, the largest variance of temperature difference is during the daytime hours, climaxing at what would usually be the peak daytime air temperature a few hours after local noon. Notice, three of the plots involving a temperature difference with the top horizontal plate 7 were similar in general profile; although, on closer inspection only Figure 5a and Figure 5b are alike. The most significant difference was for Figure 5d where the negative difference in the summer months shows a higher temperature for plate 5 over plate 6, with the reverse in winter. This is due to the difference in elevation of the sun during the summer and winter months.

The sun is highest in the sky at the local noon and thus irradiating at its maximum along over the CUBI step plates that are orientated due South. During the measurements in June and July (red and orange colors in Figure 5), the sun's maximum elevation angle was approximately  $60^{\circ}$ , while in October and November (blue and black colors) the sun's maximum elevation angle is close to  $25^{\circ}$ . This implies that in winter the plate 4 and 6 are near normal to the Sun at local noon, compared to close to grazing incident for plate 7; consequently, the energy absorbed by plate 7 is significantly lower than plates 4 and 6 explaining the strong negative temperature difference in Figure 5a and Figure 5c. We suggested a similar explanation why in summer the plate 5 is higher temperature than plate 6 during the daylight hours. Thermal infrared signature of a horizontal plate sees an unobstructed background of  $2\pi$  steradians of sky, unlike that for all the other plates; consequently, plate 7 is the simplest of the plates to model the IR signature, and provides a good reference for the other plate signatures.

Finally, if we project a smooth curved function over the top and bottom of the data creating an envelope, this would provide us a reasonable indication of the maximum temperature differences expected from these plates. In fact, it evokes the worst-case scenario for IR signature management, i.e. the maximum in the temperature differences between adjacent plates. This concept could be useful for specifying requirements, or at the least a standard comparison between data sets. The envelope function seems dominated by the solar cycle rather than environmental factors, as such, could be predicted without the requirement for a large data set.

### 3.3 Statistical analysis of the impact of day and night on the temperature differences between combinations of step plates

Having established how the temperature difference varies diurnally for each month, we now focus on the difference between daytime and nighttime. We queried the database to extract all temperature data during sunrise and sunset, representative of daytime temperatures; while, from sunset to the subsequent sunrise taken as typical of the nighttime temperatures.

We show the results of the discrete probability density of the temperature difference between the CUBI plates in the combination in Figure 6, where the left column represents the daytime while the right those during the nighttime. The determinant axis for all graphs is a difference in temperature between plates in degrees Celsius. Additionally, a side-view sketch of the CUBI highlights the relevant plates involved in the temperature difference. As for the previous figures, a graphic shows the plates used to calculate the temperature difference.

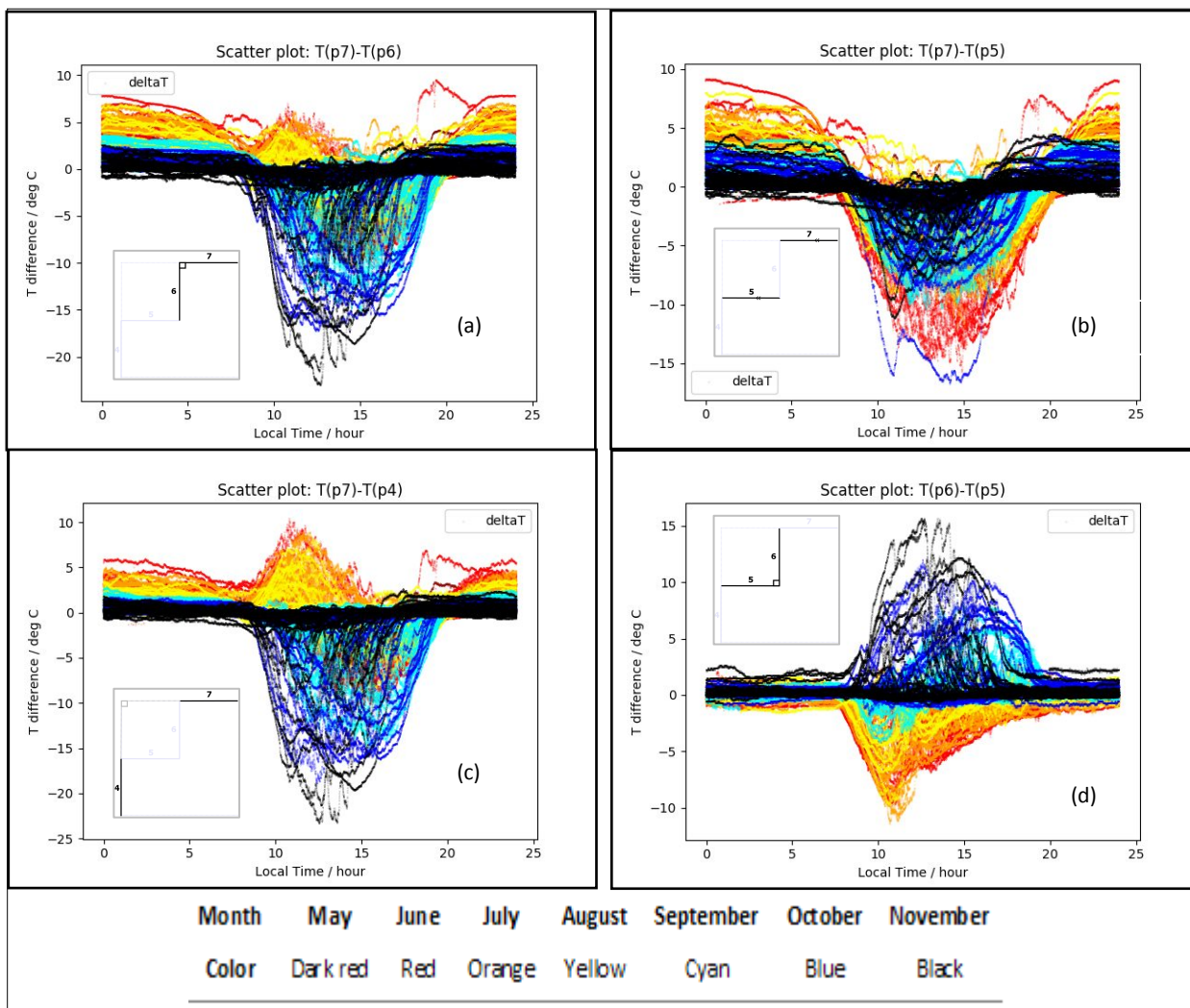


Figure 5, the variation of the temperature difference between plates along the CUBI step over the whole data from May to December 2015, representing about 180 days of measurements. Each of the colors represents data for different months. A small graphic inside the figures, shows which of the step plates are used to calculate the temperature difference.

Firstly, observe that when comparing the day and nighttime temperature difference distributions, the nighttime ones are all singled sided except for d). The latter is symmetric with a marked peak at  $0^{\circ}\text{C}$  temperature difference. Note, that during the daytime a) and b) sub-figures are very similar, while c) and d) sub-figures are also similar to each other<sup>6</sup>.



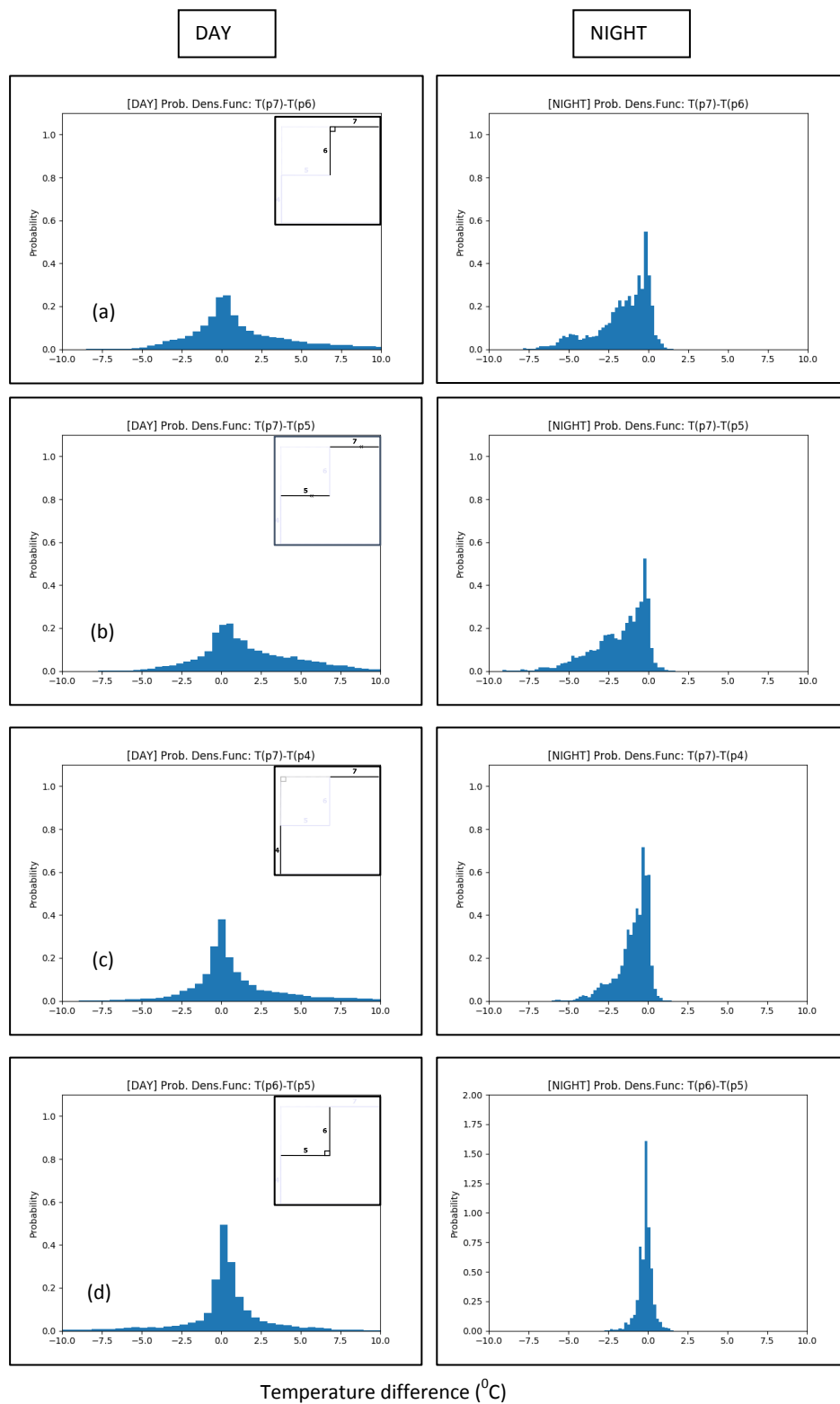


Figure 6, the discrete probability density functions day and night, for combinations of the CUBI step plates as shown by the graphics inside the figures.

If we relate our results back to the concept of IR signature management, the aim should be to reduce the contrast between the parts of the target to the point at which it appears to merge with the background clutter<sup>10</sup>. As such, we require the resulting temperature distribution over the target to be statistically similar to that of the background clutter. The apparent temperature difference is a concept common with the specifications of IR camouflage, and we show that it is an important concept for the IR signature management.

One of the principal limitations of our study, is that we only have one temperature sensor per plate albeit in the center, which is an oversimplification of the heat transfer process<sup>2,3</sup>; since, the plates do not possess infinite conductivity and consequently there is a gradient in temperature from one side to the other. In addition, temperature is important for infrared signatures, but the thermal imager detects radiance not temperature directly. Consequently, we must be prudent in our interpretation of signatures using only the surface temperatures.

#### 4. CONCLUSIONS & FURTHER RESEARCH

The purpose of this article, is to provide a statistical analysis of the measured temperature differences between the ‘L’ shaped plates of a CUBI calibration target. We demonstrated that a query-based method permits us to exploit easily the whole data set. It is noticeable that the largest fluctuations in temperature difference happen during the day due to solar heating, while at night, radiative cooling gives similar rates of temperature change for all the ‘step’ plate contributions. We trust that our analysis approach provides a useful insight for understanding the worst-case scenario for IR signature management, which may assist the development of signature standards and requirements.

We will develop a model to classify the envelope curves of temperature difference, in order to characterise to the worst-case scenario for temperature contrast. Finally, we should study the best time-periods during the day and year when the temperature difference between the plates blends naturally well with the background clutter.

#### ACKNOWLEDGMENTS

This research was funded by the Ministry of Defense of Belgium under the framework of the MRN-12 project on the infrared signature management of ships.

#### REFERENCES

- [1] Willers, C. J., Willers, M. S., Lapierre, F., Dynamics, D., Box, P. O. and Africa, S., “Signature Modelling and Radiometric Rendering Equations in Infrared Scene Simulation Systems,” Proc. SPIE **8187**, 16 (2011).
- [2] van Iersel, M., Benoist, K. W. and Cohen, L. H., “Infrared signature evolution of a CUBI,” Proc. SPIE **9614**, 9614H (2015).
- [3] Malaplate, A., Grossmann, P. and Schwenger, F., “CUBI: a test body for thermal object model validation,” Proc. SPIE **6543**, 654305 (2007).
- [4] Lewis, G. D. and Merken, P., “Investigation of the dynamic thermal infrared signatures of a calibration target instrumented with a network of 1-wire temperature sensors,” Proc. SPIE **9820**, 982010 (2016).
- [5] van Iersel, M., Veerman, H. E. T., Cohen, L. H., Benoist, K. W., van Binsbergen, S. A., van Riggelen, F. and Peet, B. J. A., “The influence of meteorological parameters on dynamic infrared signatures,” Proc. SPIE **9979**, 99790T (2016).
- [6] Jacobs, P. A., [Thermal Infrared Characterization of Ground Targets and Backgrounds, 2nd ed.], The International Society for Optical Engineering SPIE, Bellingham (2006).
- [7] Lewis, G. D. and Merken, P., “Investigation of the dynamic thermal infrared signatures of a calibration target instrumented with a network of 1-wire temperature sensors,” Proc. SPIE **9820** (2015).

- [8] Maxim Integrated., "Programmable Resolution 1-Wire Digital Thermometer" (2015).
- [9] Reinov, A., Bushlin, Y., Lessin, A. and Clement, D., "Dew , dust and wind influencing thermal signatures of objects," Proc. SPIE **6941**, 69410U (2008).
- [10] Olsen, F. B., "Methods for evaluating thermal camouflage," Brussels, Belgium (2014).